AB

UT-ICEPP 96-01
April, 1996

# Search for New Particles at LEP1.5

Contribution to Proceedings of
the Lake Louise Winter Institute (Topics in Electroweak Physics)
Alberta, CANADA, 18-24 February 1996



Shoji Asai [1] [2]

International Center for Elementary Particle Physics,
University of Tokyo
E-mail address: Shoji.Asai@cern.ch



**Abstract**

This report is summary of searches for supersymmetric particles using the recent LEP data at centre-of-mass energies of 130–140 GeV. Searches for chargino, neutralino, sleptons, and scalar top quark are discussed, and the study of $\ell^+\ell^-\mathrm{q\bar{q}}$ four fermion processes are also summarised in this report.

ICEPP

International Center for Elementary Particle Physics,

University of Tokyo

7-3-1 Hongo, Bunkyo-ku, Tokyo 113, Japan

[1]Supported by JSPS Postdoctoral Fellowships for Research Abroad
[2]Mailing address: CERN PPE-Division, CH-1211, Geneva 23, Switerland

UT-ICEPP 96-01
April, 1996

# Search for New Particles at LEP1.5

Contribution to Proceedings of
the Lake Louise Winter Institute (Topics in Electroweak Physics)
Alberta, CANADA, 18-24 February 1996

Shoji Asai [1] [2]

International Center for Elementary Particle Physics,
University of Tokyo
E-mail address: Shoji.Asai@cern.ch

**Abstract**

This report is summary of searches for supersymmetric particles using the recent LEP data at centre-of-mass energies of 130–140 GeV. Searches for chargino, neutralino, sleptons, and scalar top quark are discussed, and the study of $\ell^+\ell^-\mathrm{q\bar{q}}$ four fermion processes are also summarised in this report.

ICEPP

International Center for Elementary Particle Physics,

University of Tokyo

7-3-1 Hongo, Bunkyo-ku, Tokyo 113, Japan

[1] Supported by JSPS Postdoctoral Fellowships for Research Abroad
[2] Mailing address: CERN PPE-Division, CH-1211, Geneva 23, Switerland

# 1 Introduction

In November 1995 the LEP $e^+e^-$ collider at CERN was operated for the first time well above the Z peak at centre-of-mass energies ($\sqrt{s}$) of 130–140 GeV (LEP1.5). This provided an opportunity to search for new particles at these higher energies, but below the $e^+e^- \rightarrow W^+W^-$ threshold. In the energy region various searches could be performed at low background conditions because of the following two reasons: (1) The production cross section of the multihadronic events was smaller than the strong $Z^0$ resonance. (2) $W^+W^-$ events were absent in this energy region. $W^+W^-$ events could be the dominant background, since $W^\pm$ is a serious source of large missing transverse momentum.

Each of the four experiments ALEPH, DELPHI,L3, and OPAL had collected luminosities above 5 $pb^{-1}$ as shown in table.1. Since the luminosities at $\sqrt{s}$ = 140 GeV were very small, the data at this energy were not used for almost searches.

Table 1: Table.1 The collected luminosities at each experiment ($pb^{-1}$)

| | ALEPH | DELPHI | L3 | OPAL |
|---|---|---|---|---|
| $\sqrt{s}$=130GeV | 2.8 | 2.9 | 2.7 | 2.6 |
| $\sqrt{s}$=136GeV | 2.9 | 3.0 | 2.3 | 2.6 |
| $\sqrt{s}$=140GeV | 0.05 | 0.04 | 0.05 | 0.04 |
| TOTAL | 5.7 | 5.9 | 5.0 | 5.2 |

# 2 Search for supersymmetric particles

The supersymmetric (SUSY) standard models [1] are the most promising extensions of the standard model, because SUSY can naturally deal with the problem of the quadratic Higgs mass divergence [2]. In these theories, each elementary particle has a superpartner whose spin differs by 1/2 from that of the particle. If supersymmetry were exact, these superpartners would have the same mass as the corresponding particles. Since none of the superpartner have not yet discovered, supersymmetry must be broken.

In various SUSY theories, the Minimal Supersymmetric Standard Model (MSSM) [3] is a the simplest and the most convenient model. There are two Higgs doublet fields in the model, hence five physical Higgs bosons ($h^0$, $H^0$, $A^0$, $H^\pm$) are expected to exist. The superpartners and the Higgs bosons in this model are summarised in table 2. Charginos $\tilde{\chi}_i^\pm$ are the two mass eigenstates formed by the mixing of the fermionic partners of the charged gauge boson (winos) and those of the charged Higgs bosons (charged Higgsino). Fermionic partners of the $\gamma$, the $Z^0$ boson, and the neutral Higgs bosons mix into the four mass eigenstates

called neutralinos $\tilde{\chi}_j^0$. In both cases, the index $i$ or $j$ is ordered by increasing mass. $\tilde{\chi}_i^\pm$ and $\tilde{\chi}_j^0$ are called as "gaugino-like", when the mixing component of the gauginos is dominant, and as "Higgsino-like" in the opposite case.

Table 2: Particle list of the MSSM

| SPIN | 0 | 1/2 | 1 |
|---|---|---|---|
| neutrinos/sneutrinos | $\tilde{\nu}_L$ | $\nu_L$ | |
| leptons/sleptons | $\tilde{\ell}_L$ $\tilde{\ell}_R$ | $\ell_L$ $\ell_R$ | |
| quarks/squarks | $\tilde{q}_L$ $\tilde{q}_R$ | $q_L$ $q_R$ | |
| neutral Higgs/Higgsino | $h^0$ $H^0$ $A^0$ | $\tilde{H}_1^0$ $\tilde{H}_2^0$ | |
| gauge bosons/gauginos | | $\tilde{\gamma}$ $\tilde{Z}^0$ | $\gamma$ $Z^0$ |
| (mixing $\Rightarrow$ neutralinos) | | ($\Rightarrow$ $\tilde{\chi}_1^0$ $\tilde{\chi}_2^0$ $\tilde{\chi}_3^0$ $\tilde{\chi}_4^0$) | |
| charged Higgs/Higgsino | $H^\pm$ | $\tilde{H}^\pm$ | |
| gauge bosons/gauginos | | $\tilde{W}^\pm$ | $W^\pm$ |
| (mixing $\Rightarrow$ charginos) | | ($\Rightarrow$ $\tilde{\chi}_1^\pm$ $\tilde{\chi}_2^\pm$ ) | |
| gluons/gluinos | | $\tilde{g}_i$ ($i = 1 \sim 8$) | $g_i$ ($i = 1 \sim 8$) |

Because the supersymmetry must be broken as mentioned above, mass spectra and couplings of these superpartners depend on the choice of mechanism which breaks supersymmetry. In MSSM, soft SUSY breaking terms are inserted by hand, hence the model considered to be simply a phenomenological parameterisation. After imposing GUTs conditions, there are only five parameters in the model: $\tan\beta(\equiv v_2/v_1)$, $M_2$(universal gaugino mass), $\mu$(superpotential Higgs mass), $m_0$(universal scalar mass), and $A$(scalar trilinear coupling).

R-parity ($\equiv (-1)^{2S+3B+L}$) is defined to be even for the ordinary particles and odd for the superpartners. If R-parity is assumed to be conserved, (1) SUSY particles should be produced in pairs, (2) the lightest SUSY particle (LSP) should be stable, and (3) other SUSY particle should decay finally into the LSP and ordinary particles. The candidates for the LSP are the lightest neutralino ($\tilde{\chi}_1^0$) and sneutrino ($\tilde{\nu}$).

At LEP1.5, we searched for the following four SUSY particles: (1) $\tilde{\chi}_1^\pm$ (the lightest chargino), (2) $\tilde{\chi}_2^0$ (the second lightest neutralino), (3) $\tilde{\ell}$ (scalar leptons), and (4) $\tilde{t}_1$ (lighter state of the scalar top quark). These particles are expected to be light in general, and could be the first SUSY signal to be observed in $e^+e^-$ colliders. We assumed that the R-parity was conserved, and that the lightest neutralino $\tilde{\chi}_1^0$ was the lightest supersymmetric particle. We used the MSSM to guide the analysis but more general cases were also studied.

Furthermore there is a hot topics that the existence of light chargino and the scalar top quark could solve the reported $R_b$ anomaly. $R_b(\equiv \Gamma(Z^0 \rightarrow b\bar{b})/\Gamma(Z^0 \rightarrow q\bar{q}))$ is a value sensitive to the top quark mass, $M_t$, which is recently well measured to be $176 \pm 10$(stat.) $\pm$ 8(sys.) GeV at TEVATRON [4]. The $R_b$ measured at LEP is reported to be much larger than the standard model

prediction by more than $3\sigma$ [5]. This discrepancy is significant and could be a sign of a new physics beyond the standard model. In the several proposed solutions, the most attractive one is the supersymmetric vertex correction, in which the $\tilde{\chi}_1^{\pm}$-$\tilde{t}_1$ loops contributes to $R_b$. This correction to $R_b$ is positive, and the theoretical prediction of $R_b$ can be moved to the experimentally allowed level, if the both chargino and the scalar top quark were lighter than about 70 GeV [6].

## 2.1 The lightest chargino $\tilde{\chi}_1^{\pm}$

The charginos are the mixtures of the SUSY partner of charged Higgs boson and the SUSY partner of the $W$ boson. Previous searches at LEP 1, running at centre-of-mass energies near the $Z^0$ peak, set lower limits on the mass of the chargino at around $M_Z/2$ using a combination of direct searches and $Z^0$ width measurements [7]. A similar but more model-dependent limit was obtained by the CDF Collaboration at the TEVATRON [8].

The $\tilde{\chi}_1^{\pm}$ can be pair-produced in $e^+e^-$ collisions through $\gamma$ or $Z^0$ exchange in the $s$-channel and through sneutrino ($\tilde{\nu}$) exchange in the $t$-channel. As shown in Fig. 1 (a), the production cross section is fairly large unless the sneutrino is light, in which case destructive interference may occur between the $s$-channel and $t$-channel contributions. On the other hand, the cross section does not depend strongly on the sneutrino mass as shown in Fig. 1(b), when chargino is Higgsino-like. Because the coupling of electron-sneutrino-chargino is small in this case, the $t$-channel contribution is always suppressed.

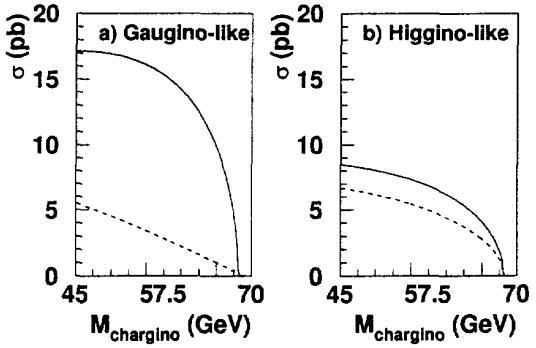


Figure 1: The production cross section of $\tilde{\chi}_1^+\tilde{\chi}_1^-$ as a function of chargino mass at $\sqrt{s}$=136GeV. (a) $\tilde{\chi}_1^{\pm}$ is gaugino-like ($\tan\beta$=1.5, $M_2$=100GeV), and (b) $\tilde{\chi}_1^{\pm}$ is Higgsino-like ($\tan\beta$=1.5, $M_2$=300GeV). The solid and dotted lines in both figures show $M_{\tilde{\nu}}$=1000GeV and 50GeV, respectively.

The details of chargino decay depend on the parameters of the mixing and the masses of the scalar partners of the ordinary fermions [9]. The lightest chargino $\tilde{\chi}_1^+$ can decay into a neutralino $\tilde{\chi}_1^0$ and a lepton pair: $\tilde{\chi}_1^+ \rightarrow \tilde{\chi}_1^0\ell^+\nu$ (leptonic

decay), or a neutralino and a quark pair: $\tilde{\chi}_1^+ \to \tilde{\chi}_1^0 q\bar{q}'$ (hadronic decay) through virtual W, slepton ($\tilde{\ell}$), or scalar quark ($\tilde{q}$) emission. The effects of the scalar quark emission are expected to be small with the assumption that scalar quarks are very heavy. In most of the MSSM parameter space, $\tilde{\chi}_1^+$ decay via the virtual W emission is dominant. However, if the $\tilde{\chi}_1^+$ is almost purely gaugino-like, and the $\tilde{\chi}_1^0$ is the almost pure SUSY partner of the $U(1)$ gauge boson, the $\tilde{\chi}_1^+$ decay via the W boson is suppressed. In such a case the dominant decay mode is $\tilde{\chi}_1^0 \ell^+ \nu$ via a virtual $\tilde{\ell}$, since the $\tilde{\ell}$ is generally lighter than the $\tilde{q}$. Therefore, it is important to search for leptonic final states as well as hadronic ones.

Figure 2 shows the distributions of the total visible energy normalised to $\sqrt{s}$ for data measured by OPAL and for the expectation of various background processes. The background processes are well simulated, and the chargino signals appear in a valley between the peak of two-photon and $q\bar{q}(\gamma)$ events in this figure, because the invisible $\tilde{\chi}_1^0$'s carry away the energy. Chargino events are also characterised by large missing transverse momentum, $P_t$, which is carried away by two $\tilde{\chi}_1^0$'s. The experimental signature for $\tilde{\chi}_1^+\tilde{\chi}_1^-$ production is therefore (a) two acoplanar leptons, (b) one lepton plus jets with large missing $P_t$, or (c) multi-jets with large missing $P_t$. At four experiments, events of these topologies were searched with the similar selection criteria.

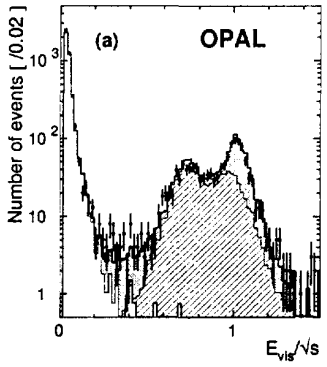


Figure 2: The distribution of the total visible energy normalised to $\sqrt{s}$ for the observed data and the Monte Carlo simulations. The hatted area indicates the production for $q\bar{q}(\gamma)$ events, the gray area for $\ell^+\ell^-(\gamma)$ events, the open area for two-photon processes and the double hated area for four fermion processes ($\nu\bar{\nu}\ell^+\ell^-$, $\nu\bar{\nu}q\bar{q}$, $\nu\ell q\bar{q}'$, $\tau^+\tau^- q\bar{q}$, $\tau^+\tau^-\tau^+\tau^-$ and $\tau^+\tau^-\mu^+\mu^-$).

No evidence of the $\tilde{\chi}_1^\pm$ was observed by all the four experiments. Because angler distribution of $\tilde{\chi}_1^\pm$ production does not depend strongly on the model-parameters, the upper limit on the production cross section can be calculated as a function of $m_{\tilde{\chi}_1^\pm}$ and $m_{\tilde{\chi}_1^0}$, assuming a particular decay-mode. Figure 3 (a) and (b) show the obtained upper limits on the production cross section of $\tilde{\chi}_1^\pm$, when $\tilde{\chi}_1^\pm$ decays into $\tilde{\chi}_1^0$ plus W*-boson, and into $\tilde{\chi}_1^0$ plus $\ell\nu$, respectively. The $\tilde{\chi}_1^\pm$ masses smaller than 68 GeV are excluded at 95% confidence level, if the cross section is larger than 3 pb and the mass difference between $\tilde{\chi}_1^\pm$ and $\tilde{\chi}_1^0$ is larger than 10 GeV, and if $\tilde{\chi}_1^\pm$ decays into $\tilde{\chi}_1^0$ plus W*-boson only.

Since the production cross section and decay branching fraction of $\tilde{\chi}_1^\pm$ can be calculated using the MSSM, the lower limit on the $\tilde{\chi}_1^\pm$-mass can be obtained within the restricted parameter space as summarised in table 3. The limits depend on the $M_{\tilde{\nu}}$ because of the negative interference of the $s$- and $t$-channel.

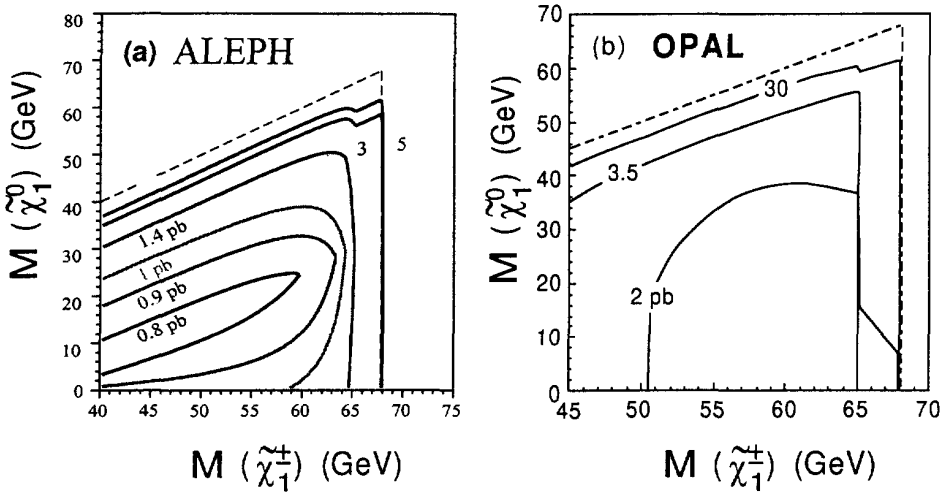


Figure 3: 95 % CL upper limits on the $\tilde{\chi}_1^\pm$ production cross section (pb) at $\sqrt{s}$=136 GeV. $\tilde{\chi}_1^\pm$ is assumed to decay into: (a) $\tilde{\chi}_1^0$ plus W*-boson [11], and (b) $\tilde{\chi}_1^0$ plus $\ell\nu$ [10].

Table 3: 95 % CL lower limits on $\tilde{\chi}_1^\pm$-mass (DELPHI Preliminary)

| lower limits on $\tilde{\chi}_1^\pm$-mass | Assumption on $M_{\tilde{\nu}}$ | Constrain on the MSSM-parameters |
|---|---|---|
| 65.8 GeV | $M_{\tilde{\nu}} = 1000$ GeV | $\tan\beta$=1,1.5,50<br>$0 \leq M_2 \leq 800$ GeV<br>$-400 \leq \mu \leq 400$ GeV<br>$m_{\tilde{\chi}_1^\pm} - m_{\tilde{\chi}_1^0} \geq 10$ GeV |
| 56.3 GeV | $41 \leq M_{\tilde{\nu}} \leq 1000$ GeV | |

## 2.2 The second lightest neutralino $\tilde{\chi}_2^0$

The neutralinos are the mixtures of the SUSY partners of neutral Higgs bosons and the SUSY partners of neutral gauge bosons. The $\tilde{\chi}_1^0\tilde{\chi}_2^0$ can be co-pair produced by an $s$-channel virtual $Z^0$ exchange or $t$-channel scalar electron ($\tilde{e}$) exchange, if $m_{\tilde{\chi}_1^0} + m_{\tilde{\chi}_2^0}$ is smaller than $\sqrt{s}$. This associate production could give the first direct signal for neutralinos, since single photon events from $e^+e^- \to \tilde{\chi}_1^0\tilde{\chi}_1^0\gamma$ suffer from background process of $e^+e^- \to \nu\bar{\nu}\gamma$ in the LEP1.5 energy region. When both $\tilde{\chi}_1^0$ and $\tilde{\chi}_2^0$ are Higgsino-like ($|\mu| \ll M_2$), the $s$-channel contribution plays important role, and the cross section of about a few pb is expected.

If the $\tilde{\chi}_2^0$ is the lightest visible SUSY particle, $\tilde{\chi}_2^0$ would decay into $\tilde{\chi}_1^0\ell^+\ell^-$, $\tilde{\chi}_1^0\nu\bar{\nu}$, or $\tilde{\chi}_1^0 q\bar{q}$ through a virtual $Z^0$, Higgs boson, sleptons, or squarks. Except for the invisible case of $\tilde{\chi}_2^0 \to \tilde{\chi}_1^0\nu\bar{\nu}$, the event topologies of $\tilde{\chi}_1^0\tilde{\chi}_2^0$ are similar to $\tilde{\chi}_1^+\tilde{\chi}_1^-$ events. Then $\tilde{\chi}_1^0\tilde{\chi}_2^0$ events were searched with the selection criteria similar to the chargino search.

No evidence of $\tilde{\chi}_1^0\tilde{\chi}_2^0$ events were also observed at all experiments. Figure 4 shows the obtained upper limits on the production cross section of $\tilde{\chi}_1^0\tilde{\chi}_2^0$, when $\tilde{\chi}_2^0$ decays into $\tilde{\chi}_1^0$ plus a virtual $Z^0$-boson.

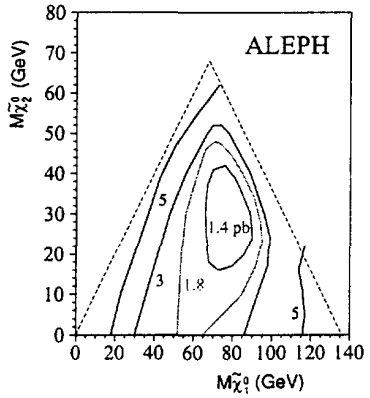


Figure 4: 95 % CL upper limits on the $\tilde{\chi}_1^0\tilde{\chi}_2^0$ associate production cross section (pb) at $\sqrt{s}$=136GeV [11]. $\tilde{\chi}_2^0$ is assumed to decay into $\tilde{\chi}_1^0$ plus a virtual $Z^0$.

In the MSSM, production cross sections and decay branching fractions of charginos and neutralinos are determined by the four MSSM-parameters; $M_2$, $\mu$, $\tan\beta$, and $m_0$. In the regions where $\tilde{\chi}_1^+\tilde{\chi}_1^-$ production is suppressed, SUSY signatures can be explored via $\tilde{\chi}_1^0\tilde{\chi}_2^0$ associate production. The limits on the MSSM-parameters presented here is therefore based on combining both the neutralino and chargino searches.

Figure 5 shows the excluded region in the $M_2$-$\mu$ plane for the case $m_0$=1 TeV (Fig. 5(a)) and the lightest $m_0$ (Fig. 5(b)) with $\tan\beta$=1.5. The same plots are shown with $\tan\beta$=35 (Fig. 5(c) and (d)).

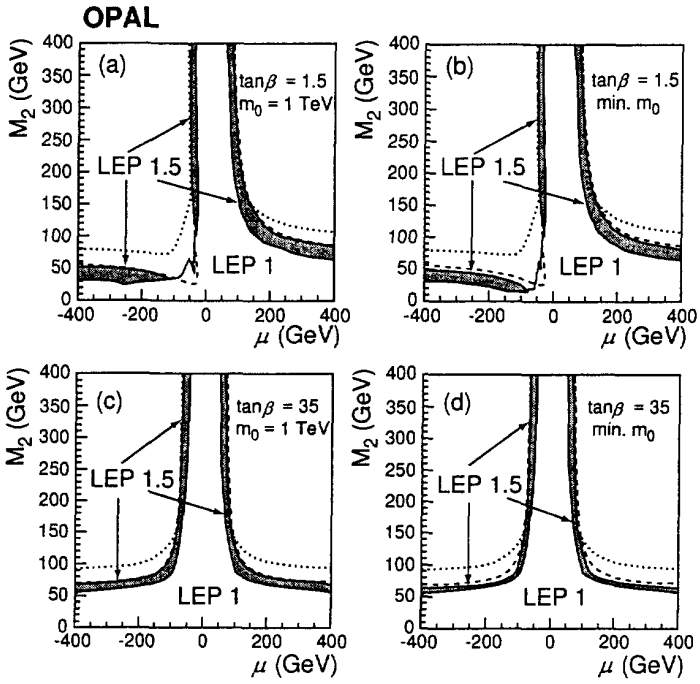


Figure 5: The excluded regions in $M_2$-$\mu$ plane for the case (a) $m_0$=1 TeV and (b) the lightest $m_0$ with $\tan\beta$=1.5. The same plots are shown for $\tan\beta$=35 ((c) and (d)). The lightest $m_0$ is defined to be the smallest $m_0$ possible to comply with the limits on $\tilde{\ell}$ and $\tilde{\nu}$ at LEP1. The regions labelled as "LEP1" had been already excluded by the analysis of LEP1 data. The dashed and dotted lines in these figures show the kinematical boundary at $\sqrt{s}$=136GeV for $\tilde{\chi}_1^+\tilde{\chi}_1^-$ and $\tilde{\chi}_1^0\tilde{\chi}_2^0$, respectively.

Most of the excluded regions are due to the results of the $\tilde{\chi}_1^+\tilde{\chi}_1^-$ search. The $\tilde{\chi}_1^0\tilde{\chi}_2^0$ search contributes only in the limited area near the kinematical boundary of the $M_2 \gg |\mu|$ region. As mentioned above, the parameters are excluded almost up to the $\tilde{\chi}_1^+\tilde{\chi}_1^-$ kinematical boundary, when $m_0$ is 1 TeV. On the other hand, there are gaps between the excluded regions and the $\tilde{\chi}_1^+\tilde{\chi}_1^-$ kinematical boundary, if $m_0$ is very small.

## 2.3 Sleptons

The sleptons (selectrons $\tilde{e}$, smuons $\tilde{\mu}$, and staus $\tilde{\tau}$) are the SUSY partners of the leptons. Sleptons are classified into "right-handed" or "left-handed" sleptons, depending on the helicity to which they are associated. The right-handed slepton are always lighter than the same flavour left-handed sleptons in the MSSM. Previous searches for sleptons at LEP 1 set lower limits on the slepton mass at 45 GeV [12].

Slepton is pair produced by $s$-channel $Z^0$ and $\gamma$ exchange. The selectron is also pair produced by $t$-channel neutralino exchange. Since production cross section of the right-handed sleptons are lower than that of the left-handed as shown in Fig. 6, the expected number of the slepton events are conservatively calculated by considering only right-handed sleptons. The production cross section of the right-handed smuon and stau is smaller than 0.7 pb as shown in this figure.

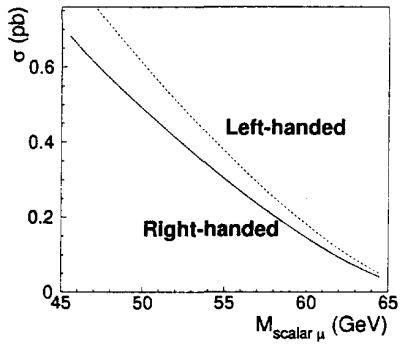


Figure 6: The production cross section of $\tilde{\mu}^+\tilde{\mu}^-$ as a function of $\tilde{\mu}$ mass at $\sqrt{s}$=136GeV. The solid and dotted lines are for $\tilde{\mu}_R^+\tilde{\mu}_R^-$ and $\tilde{\mu}_L^+\tilde{\mu}_L^-$, respectively.

Typical cross sections of the right-handed selectron, $\tilde{e}_R$, are listed in the next table. The $t$-channel contribution substantially enhances the $\tilde{e}_R$ production cross section, when the lightest neutralino $\tilde{\chi}_1^0$ is light and gaugino-like.

Table 4: The production cross sections of the right-handed selectron at $\sqrt{s}$=136 GeV. ($\tan\beta$=1.5 and $\mu = -200$ GeV)

| $\sigma(e^+e^- \to \tilde{e}_R^+\tilde{e}_R^-)$ | $m_{\tilde{\chi}_1^0} = 40$ GeV | $m_{\tilde{\chi}_1^0} = 23$ GeV |
|---|---|---|
| $m_{\tilde{e}_R} = 50$ GeV | 2.02 pb | 3.26 pb |
| $m_{\tilde{e}_R} = 55$ GeV | 0.95 pb | 1.92 pb |
| $m_{\tilde{e}_R} = 60$ GeV | 0.24 pb | 0.86 pb |

The right-handed slepton $\tilde{\ell}_R$ decays into the $\tilde{\chi}_1^0$ plus the corresponding ordinary lepton $\ell$. Therefore the events topology of $\tilde{\ell}_R^+\tilde{\ell}_R^-$ pair-production is acoplanar lepton pair with the large missing transverse momentum. This topology is similar to the leptonic decay of chargino, and the selection criteria similar to the chargino search were used.

For all the lepton flavours, no evidence of the sleptons was observed by all the experiments. Figure 7 shows the upper limits on the production cross section of $\tilde{\ell}^+\tilde{\ell}^-$ for each flavour. Selectron $\tilde{e}$ and smuon $\tilde{\mu}$ are excluded, when the production cross section is larger than 3 pb and the mass difference between $\tilde{\ell}$ and $\tilde{\chi}_1^0$ is larger than 5 GeV [13]. When the mass difference is smaller than 10 GeV, the total visible energy of $\tilde{\tau}^+\tilde{\tau}^-$ event is very small, and it is difficult to distinguish this signal from the two-photon background events. Then the obtained limits for $\tilde{\tau}$ become worse.

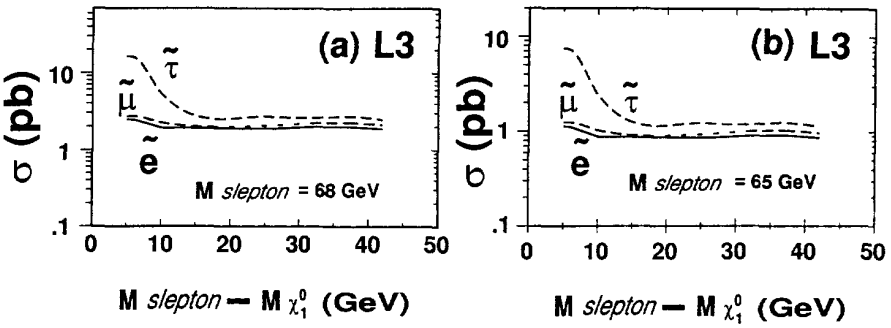


Figure 7: 95 % CL upper limits on the production cross section of $\tilde{\ell}^+\tilde{\ell}^-$ as a functions of the mass difference between $\tilde{\ell}^{\pm}$ and $\tilde{\chi}_1^0$. (a) $m_{\tilde{l}^{\pm}} = 68$ GeV at $\sqrt{s}$=136 GeV, (b) $m_{\tilde{l}^{\pm}} = 65$ GeV at $\sqrt{s}$=130 GeV.

Since the production cross section of $\tilde{\mu}_R$ and $\tilde{\tau}_R$ is smaller than 0.7 pb as already shown in Fig. 6, we can not improve the lower limits on the mass of $\tilde{\mu}$ and $\tilde{\tau}$. For selectrons, Fig. 8 shows the 95 % CL excluded region of $\tilde{e}_R$ in the ($m_{\tilde{e}_R}$-$m_{\tilde{\chi}_1^0}$) plane. The lower limit on $m_{\tilde{e}_R}$ is obtained to be 52 GeV, when the mass difference between $\tilde{e}_R$ and $\tilde{\chi}_1^0$ is larger than 10 GeV.

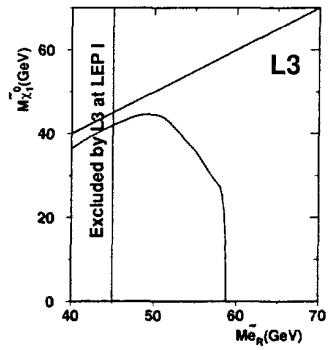


Figure 8: 95 % CL excluded region in the $m_{\tilde{e}_R}$-$m_{\tilde{\chi}_1^0}$ plane, with $\tan\beta$=1.5. The MSSM parameters are restricted within $M_2 < 200$ GeV, $|\mu| < 200$ GeV, and $m_0 < 100$ GeV. The region of $m_{\tilde{e}_R} < 45$ GeV had been excluded by searches at LEP1.

## 2.4 Scalar top quark

The scalar top quark ($\tilde{t}$), the bosonic partner of the top quark, can be the lightest charged supersymmetric (SUSY) particle for two reasons [14, 15]. Firstly, one loop radiative corrections to the $\tilde{t}$ mass through Higgsino-quark loops and Higgs-squark loops are always negative. The correction is large because of the heavy top quark mass. Secondly, the supersymmetric partners of the right-handed and left-handed top quarks ($\tilde{t}_L$ and $\tilde{t}_R$) mix, and the resultant two mass eigenstates

($\tilde{t}_1$ and $\tilde{t}_2$) have a large mass splitting. The lighter mass eigenstate ($\tilde{t}_1$) can be lighter than any other charged SUSY particle, and lighter than the top quark itself. The $\tilde{t}_1$ mass, $m_{\tilde{t}_1}$, can be also close to that of the lightest neutralino $\tilde{\chi}^0_1$.

Lower limits on scalar quark masses have been obtained from $p\bar{p}$ colliders [16], assuming that all the scalar quark masses of the five or six flavours are degenerate, and that the masses of the left and right-handed partners are equal. Such assumptions are invalid for the $\tilde{t}_1$. Recently the D0 Collaboration reported a lower limit [17] on the $\tilde{t}_1$ mass of about 100 GeV in the case where the mass difference between $\tilde{t}_1$ and $\tilde{\chi}^0_1$ is larger than about 35 GeV. Searches at $e^+e^-$ colliders are sensitive to a smaller mass difference, and lower limits for the $\tilde{t}_1$ mass have been obtained at the $Z^0$ peak [18, 19].

Scalar top quark pairs, $\tilde{t}_1\bar{\tilde{t}}_1$, could be produced in $e^+e^-$ annihilation via a virtual $Z^0$ boson or a virtual photon. As shown in Fig. 9, the total cross section including both the first order QCD and QED corrections has been calculated [14] as a function of the scalar top mass, $m_{\tilde{t}_1}$, and the mixing angle, $\theta_{\rm mix}$, where $\theta_{\rm mix}$ is defined by $\tilde{t}_1 = \tilde{t}_{\rm L}\cos\theta_{\rm mix} + \tilde{t}_{\rm R}\sin\theta_{\rm mix}$. The coupling between the $\tilde{t}_1$ and the $Z^0$ boson depends on the mixing angle, which is determined by the top quark mass and the soft SUSY breaking parameters. For $\theta_{\rm mix}$ close to 0.98 ($\cos^2\theta_{\rm mix} = \frac{4}{3}\sin^2\overline{\theta_{\rm W}}$), $\tilde{t}_1$ decouples from the $Z^0$ boson, and $\tilde{t}_1\bar{\tilde{t}}_1$ can be produced only via a virtual $\gamma$.

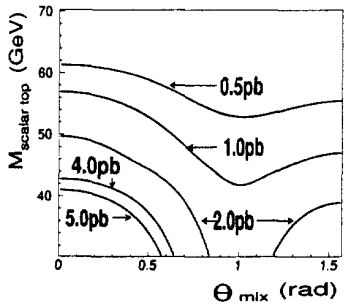


Figure 9: The production cross section of $\tilde{t}_1\bar{\tilde{t}}_1$ at $\sqrt{s}$=136GeV as a function of the mixing angle $\theta_{\rm mix}$ and $\tilde{t}_1$ mass.

If the chargino $\tilde{\chi}^\pm_1$ is lighter than $m_{\tilde{t}_1} - m_b$ where $m_b$ is bottom quark mass, then $\tilde{t}_1 \to b\tilde{\chi}^\pm_1$ would be the dominant decay. However, this decay mode is not considered in this study, since a $\tilde{\chi}^\pm_1$ lighter than 56.3 GeV is already excluded as mentioned in section 2.1. In addition, the scalar neutrino $\tilde{\nu}$ and the scalar lepton $\tilde{\ell}$ are assumed to be heavier than the $\tilde{t}_1$. In such a case, the dominant decay mode of the $\tilde{t}_1$ is restricted to be the simple two body decay: $\tilde{t}_1 \to c\tilde{\chi}^0_1$ via one-loop processes [14]. Because the lifetime of the $\tilde{t}_1$ is much longer than the typical time scale of the hadronisation, the $\tilde{t}_1$ would hadronise to form a $\tilde{t}_1$-hadron before it decays. The experimental signature for $\tilde{t}_1\bar{\tilde{t}}_1$ events is an acoplanar two-jet topology with large transverse momentum, which is similar to the chargino hadronic decay.

No event of $\tilde{t}_1\bar{\tilde{t}}_1$ was observed at all the four experiments. Figure 10 shows 95 % CL excluded region in $\theta_{\rm mix}$-$m_{\tilde{t}_1}$ plane, when the mass difference between $\tilde{t}_1$ and $\tilde{\chi}^0_1$ is larger than 5 GeV. The lower limit on $m_{\tilde{t}_1}$ is obtained to be 52.4 GeV in the case of $\theta_{\rm mix}$=0.0. The excluded region in $m_{\tilde{t}_1}$-$m_{\tilde{\chi}^0_1}$ plane is also shown in this figure, in which the mixing angle $\theta_{\rm mix}$ is assumed to be 0.0.

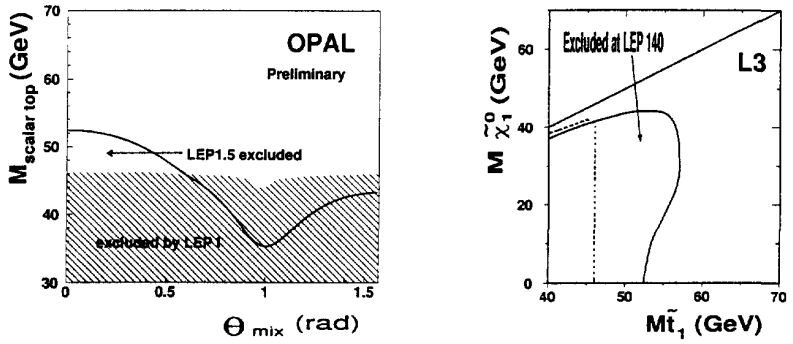


Figure 10: (Left side): 95 % CL excluded region in $\theta_{\rm mix}$-$m_{\tilde{t}_1}$ plane, when the mass difference between $\tilde{t}_1$ and $\tilde{\chi}^0_1$ is larger than 5 GeV. The hatted area indicates the excluded regions by searches at LEP1. (Right side): 95 % CL excluded region in $m_{\tilde{t}_1}$-$m_{\tilde{\chi}^0_1}$ plane, when the mixing angle $\theta_{\rm mix}$ is 0.0. The dotted line indicates the excluded regions by searches at LEP1.

# 3 Four fermion processes

Four fermion processes are production processes of two fermion-antifermion pairs in $e^+e^-$ collisions, and these are the standard processes described by the Standard Model. These processes become more serious and sizable background for new particles including Higgs searches as higher the beam energy. In the SUSY searches at LEP1.5, the four fermion processes in which at least one of the fermions was a neutrino ($\nu\bar{\nu}\ell^+\ell^-$, $\nu\bar{\nu}q\bar{q}$, and $\nu\ell q\bar{q}'$) were well studied at the four experiments. The prediction by the standard model agreed with the observed data within the statistical errors. The other final state of $\ell^+\ell^-q\bar{q}$ ($\ell$ = e,$\mu$) processes were also studied [20] in the OPAL experiment. In this section, I briefly summarise this result.

The $\ell^+\ell^-q\bar{q}$ processes at LEP1.5 emerge from neutral bosons, i.e. virtual photons and real or virtual Z bosons. In the case of electrons in the final state there are also contributions from $t$-channel boson exchange. Figure 11 shows the diagrams contribute to this final state, and dominant diagrams depend on $\sqrt{s}$. At LEP1.5, "conversion" diagrams are dominating, especially diagram(C), because there is a strong resonance at $M_{q\bar{q}} \sim M_{Z^0}$. When the initial state radiations are taken into account, the contribution of "annihilation" diagrams (diagram(B)) is also sizable, because the intermediate $Z^0$ can be on-shell state. "Bremsstrahlung"

and "multiperipheral" contribute only to $e^+e^-q\bar{q}$ final state. But most of $e^+$ or $e^-$ escape into beam pipe, these contributions are expected to be very small.

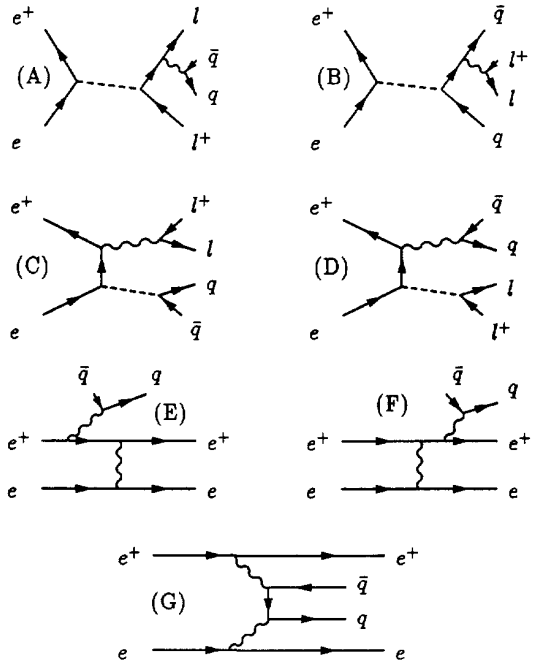


Figure 11: Schematic Feynman diagrams for the four-fermion production process $e^+e^- \rightarrow \ell^+\ell^-q\bar{q}$, divided into the four gauge-invariant groups: annihilation (A,B), conversion (C,D), bremsstrahlung (E,F) and multiperipheral (G) diagrams. The dashed line symbolises an intermediate $\gamma$ or Z boson. The contribution of the respective diagrams is especially high if the Z boson is on its mass shell. In addition all photon lines can also be replaced by a $Z^0$.

The $e^+e^-q\bar{q}$ and $\mu^+\mu^-q\bar{q}$ processes were generated with the FERMISV program [21]. The fragmentation of the two final state quarks was handled by JETSET 7.4 with parameters tuned for multihadronic decays of the $Z^0$. The main physics background to the $\ell^+\ell^-q\bar{q}$ final state came from multihadronic events with two relatively isolated leptons. These could arise either from semileptonic decays of heavy quarks, or in the case of electron pairs from a converted initial state photon. Multihadronic events were simulated with JETSET 7.4 and PYTHIA 5.7.

In order to select the hadronic events with the isolated lepton pair, the following selections were used:

- The number of charged tracks was required to be at least six.
- The number of jets had to be greater than or equal to two. Jets were reconstructed using the Durham algorithm [22] with $x^2_{min} = 49$ GeV$^2$.

- Leptons were identified. Lepton candidates were required to have a momentum $p \geq 5$ GeV/$c$. A track was classified as an electron if the ratio $E/p$ was greater than 0.8, where $p$ was the track momentum and $E$ the associated electromagnetic energy. Furthermore the energy loss $\mathrm{d}E/\mathrm{d}x$ in the central tracking chamber had to be within a range of values where 99% of the electrons with this momentum were expected. Muons were required to have $E/p < 0.2$ and at least three hits in the muon chambers or the last three layers of the hadronic calorimeter.

- For each lepton candidate an isolation angle $\alpha^{\mathrm{iso}}$ was defined as the maximum angle at which the energy $E_{\mathrm{cone}}$ contained within a cone of half-angle $\alpha^{\mathrm{iso}}$ around the lepton was less than 1 GeV. In order to keep events with low-mass lepton pairs, $E_{\mathrm{cone}}$ was defined to be the energy of all tracks and unassociated electromagnetic clusters within the cone, excluding both the lepton candidate itself, and also the nearest other lepton candidate if it lay within the cone.

- The two most isolated leptons of each flavour were regarded as a candidate lepton pair. If the charges of the leptons were of the same sign, the event was rejected. Their momenta and isolation angles were called $p_i$, $i = 1, 2$ and $\alpha_i^{\mathrm{iso}}$, respectively, where $i = 1$ designated the lepton having the larger isolation angle.

- We exploited the isolation of the lepton candidates mentioned above, $\alpha_1^{\mathrm{iso}} \geq 30^\circ$, $\alpha_2^{\mathrm{iso}} \geq 10^\circ$ and $|p_1| + |p_2| \geq 15$ GeV.

- In order to reject photon conversions for $\mathrm{e^+e^-q\bar{q}}$ events, a invariant mass of the electron pair was demeaned to be larger than 1 GeV.

After these selections, 2 events were observed for the $\mathrm{e^+e^-q\bar{q}}$ candidate, and 5 events for the $\mu^+\mu^-\mathrm{q\bar{q}}$ candidate. The expected number and contributions of background processes are summarised in table 5. "Contribution from colour octet quarkonium" is a hypothetical background arises from colour octet isolated quarkonium production from single hard gluon emission from quarks in multihadronic events. This model was introduced recently to explain the larger charmonium and bottomonium production cross sections observed by CDF [23]. It is also consistent with the recent OPAL observation of $\Upsilon$ production in $\mathrm{Z^0}$ decays [24].

The systematic errors of this analysis are also summarised in the table. 6. We have cross-checked the prediction of the FERMISV against that of the the EXCALIBUR, and the same number of events are predicted within the statistical uncertainty. Total systematic error was calculated as a quadratic sum of the individual errors, since these systematic errors were considered to be independent. As shown in this table, the systematic errors are well controlled, and this value is same size as the statistical errors presented in table 5.

A significant discrepancy between the SM prediction and the detected number is observed in the $\mu^+\mu^-\mathrm{q\bar{q}}$ processes. The Poisson probability for this excess is

Table 5: Final results for number of the expected and observed events.

| | $e^+e^-q\bar{q}$ | $\mu^+\mu^-q\bar{q}$ |
|---|---|---|
| Signal of $\ell^+\ell^-q\bar{q}$ (FERMISV) | 0.66 | 0.51 |
| $e^+e^- \rightarrow ff$ background | 0.28 | 0.11 |
| the other four fermion processes | 0.07 | 0.02 |
| Contribution from colour octet quarkonium | 0.01 | 0.01 |
| Total expected number | $1.02 \pm 0.14$ | $0.65 \pm 0.08$ |
| Number of the observed event | 2 | 5 |

Table 6: Systematic error sources and these contribution to the final results

| Source | $e^+e^-q\bar{q}$ | $\mu^+\mu^-q\bar{q}$ |
|---|---|---|
| Generator dependence (FERMISV vs EXCALIBUR) | consistent within statistical error | |
| Higher order correction to FERMISV | $\pm$ 0.10 | $\pm$ 0.05 |
| Background estimation ($e^+e^- \rightarrow ff$) | $\pm$ 0.14 | +0.11 -0.05 |
| Background estimation (the other 4-fermion) | $\pm$ 0.03 | $\pm$ 0.01 |
| Colour octet quarkonium | $\pm$ 0.01 | $\pm$ 0.01 |
| Total systematic error | $\pm$ 0.17 | +0.12 -0.07 |

0.26 %, if the origin of this excess is considered to be statistical fluctuation. While one would expect peaks in either the invariant mass of leptonic system or the hadronic system, if the observed excess were due to a leptonic or hadronic resonance, not present in the Monte Carlo simulations. Figure 12 shows the distribution of the invariant mass of the hadronic system, which should be the same value as the recoil mass of the lepton system. For events from diagram(C) the invariant mass of the hadronic system peaks at the $Z^0$ mass, and that of the leptonic system which comes from a virtual photon peaks at small invariant mass. The configuration of the mass values is vice-versa for the events from diagram(D). As shown in Fig. 12 (b), this excess is observed at $M_{q\bar{q}} \sim M_{Z^0}$. No additional peak is seen in this data, and no significant deviations in the shapes of differential distributions from the SM prediction are observed. We can not understand the origin of this excess.

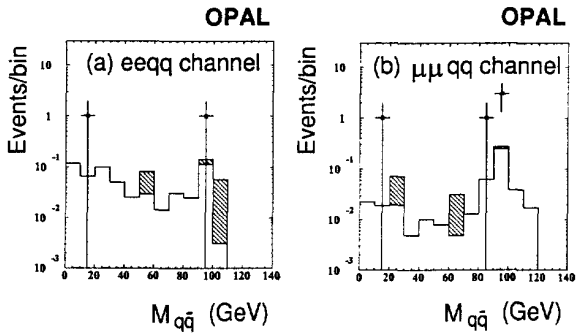


Figure 12: Distribution of the invariant mass of $q\bar{q}$ system for the selected events. The open histograms in both figures show the $\ell^+\ell^- q\bar{q}$ signal predictions, and the hatted histograms represent the distribution of the background process.

# 4 Conclusion

The LEP collider was operated at centre-of-mass energies of 130–140 GeV, and each of the four experiments had collected luminosities above 5 $pb^{-1}$. Using these data, we searched for the various SUSY particles: the lightest chargino $\tilde{\chi}_1^{\pm}$, the second lightest neutralino $\tilde{\chi}_2^0$, the sleptons $\tilde{\ell}^{\pm}$, and the lighter state of the scalar top quark $\tilde{t}_1$. These particles are expected to be light and could give the first direct signal for SUSY. No evidence for SUSY was observed and the lower limits on the masses of these particles were improved. The typical obtained limits are listed in table 7. These are well above the limits obtained at LEP-1, running at centre-of-mass energies near the $Z^0$ peak.

The $\tilde{\chi}_1^{\pm}$-$\tilde{t}_1$ loops contribute to $R_b$ is re-examined with these obtained limits, and this contribution $R_b^{SUSY}$ is found to be smaller than 0.0017 [26] in the MSSM. Such values of $R_b^{SUSY}$ tend to disfavour that the current $R_b$ anomaly is explained only by the SUSY contributions.

Table 7: The Obtained lower limits on masses of the SUSY particles.

| | Assumptions |
|---|---|
| $m_{\tilde{\chi}_1^{\pm}} > 65.8$ GeV | MSSM, $\tan\beta = 1 \sim 50$<br>$\|\mu\| < 400$ GeV<br>$M_2 < 400$ GeV<br>$m_{\tilde{\nu}} = 1$ TeV<br>$m_{\tilde{\chi}_1^{\pm}} - m_{\tilde{\chi}_1^0} > 10$ GeV |
| $m_{\tilde{\chi}_2^0} > 69$ GeV | MSSM<br>$\tilde{\chi}_2^0$ is Higgsino-like<br>$m_{\tilde{\chi}_2^0} - m_{\tilde{\chi}_1^0} > 10$ GeV |
| $m_{\tilde{e}_R^{\pm}} > 52$ GeV | MSSM, $\tan\beta = 1.5$<br>$\|\mu\| < 200$ GeV<br>$M_2 < 200$ GeV<br>$m_0 < 100$ GeV<br>$m_{\tilde{e}_R^{\pm}} - m_{\tilde{\chi}_1^0} > 10$ GeV |
| $m_{\tilde{t}_1} > 55.5$ GeV | $\theta_{mix} = 0$<br>$m_{\tilde{t}_1} - m_{\tilde{\chi}_1^0} > 10$ GeV |

The $\ell^+\ell^-q\bar{q}$ ($\ell = e, \mu$) four fermion processes were also studied using these high energy data. OPAL reported the excess above the SM prediction in the $\mu^+\mu^-q\bar{q}$ process, but no significant deviations in the shapes of differential distributions from the SM prediction were observed. The Poisson probability for this excess is 0.26 %, if the origin of this excess is considered to be statistical fluctuation.

# Acknowledgements

It is a pleasure to thank the SL Division for efficient operation of the LEP accelerator at the new energies of $\sqrt{s}$=130-140GeV with good beam conditions. I also would like to thank the LEP collaborations ALEPH, DELPHI, L3, and OPAL for making their latest physics results available in the Lake Louise Winter Institute. In particular I would like to acknowledge Sachio Komamiya (OPAL), Jean-Francois Grivaz (ALEPH), Michael Schmitt (ALEPH), Pierpaolo Rebecchi (DELPHI), Anna Lipniacka (DELPHI), Marta Felcini (L3), Andre Sopczak (L3), Hans-Christian Schultz-Coulon (OPAL), and Michael Kobel (OPAL). Finally, I would like to thank the organisers of the Winter Institute who provide us nice skiing conditions including the nice weather.

# References

[1] Y. Gol'fand and E. Likhtam, JETP Lett. **13** (1971) 323;
D. Volkov and V. Akulov, Phys. Lett. **B46** (1973) 109;
J. Wess and B. Zumino, Nucl. Phys. **B70** (1974) 39.

[2] M. Veltman, Acta Phys. Pol. **B8** (1977) 475.

[3] H. P. Nilles, Phys. Rep. **110** (1984) 1;
H. E. Haber and G. L. Kane, Phys. Rep. **117** (1985) 75.

[4] CDF Collaboration, F. Abe *et al.*, Phys. Rev. **D52** (1995) 2605;
D0 Collaboration, S. Abachi *et al.*, Phys. Rev. **D52** (1995) 4877.

[5] The LEP Collaborations ALEPH, DELPHI, L3 and OPAL, CERN-PPE/95-172 (1995).

[6] G. L. Kane, R. G. Stuart, and J. D. Wells, UM-TH-94-16, hep-ph/9505207 (1995);
J. D. Wells, C. Kolda, and G. L. Kane, UM-TH-94-23, hep-ph/9408228 (1994).

[7] L3 Collab., B. Adeva *et al.*, Phys. Lett. **B233** (1989) 530;
ALEPH Collab., D. Decamp *et al.*, Phys. Lett. **B236** (1990) 86;
OPAL Collab., M.Z. Akrawy *et al.*, Phys. Lett. **B240** (1990) 261;
DELPHI Collab., P. Abreu *et al.*, Phys. Lett. **B247** (1990) 157;
ALEPH Collab., D. Decamp *et al.*, Phys. Rep. **216** (1992) 253.

[8] CDF Collab., J. Hauser, in the Proc. of the 10th Topical Workshop on Proton-Antiproton Collider Physics, Fermilab, IL, USA, May 1995.

[9] A. Bartl, H. Fraas and W. Majerotto, Z. Phys. **C30** (1986) 441;
A. Bartl, H. Fraas and W. Majerotto, Z. Phys. **C41** (1988) 475;
A. Bartl, H. Fraas, W. Majerotto and B. Mösslacher, Z. Phys. **C55** (1992)

257;
M. Chen, C. Dionisi, M. Martinez and X. Tata, Phys. Rep. **159** (1988) 201;
J. L. Feng and M. J. Strassler, Phys. Rev. **D51** (1995) 4661.

[10] OPAL Collab., G. Alexander *et al.*, CERN-PPE/96-20 (1996), Accepted by Phys. Lett. B.

[11] ALEPH Collaboration, D. Buskulic *et al.*, CERN-PPE/96-10 (1996), Submitted to Phys. Lett. B.

[12] ALEPH Collaboration, D. Decamp *et al.*, Phys. Rep. **216** (1992) 253.

[13] L3 Collab., M. Acciarri *et al.*, CERN-PPE/96-29 (1996), Submitted to Phys. Lett. B.

[14] M. Drees and K. Hikasa, Phys. Lett. **B252** (1990) 127;
K. Hikasa and M. Kobayashi, Phys. Rev. **D36** (1987) 724.

[15] J. Ellis and S. Rudaz, Phys. Lett. **B128** (1983) 248;
G. Altarelli and R. Rückl, Phys. Lett. **B144** (1984) 126;
S. Dawson, E. Eichten and C. Quigg, Phys. Rev. **D31** (1985) 1581;
J. Ellis, G.L. Fogli and E. Lisi, Nucl. Phys. **B393** (1993) 3.

[16] UA1 Collaboration, C. Albajar *et al.*, Phys. Lett. **B198** (1987) 261;
UA2 Collaboration, J. Alitti *et al.*, Phys. Lett. **B235** (1990) 363;
H.Baer, X. Tata and J. Woodside, Phys. Rev. **D44** (1991) 207;
D0 Collaboration, F. Abachi *et al.*, Phys. Rev. Lett. **75** (1995) 618.

[17] D0 Collaboration, F. Abachi *et al.*, FERMILAB-PUB-95-380-E (1995), Accepted by Phys. Rev. Lett.

[18] OPAL Collab., R. Akers *et al.*, Phys. Lett. **B337** (1994) 207.

[19] ALEPH Collaboration, International Europhysics Conference on High Energy Physics, Brussels, Belgium, 27 July - 2 August (1995).

[20] OPAL Collab., G. Alexander *et al.*, CERN-PPE/96-31 (1996), submitted to Phys. Lett. B.

[21] J. Hilgart, R. Kleiss and F. Le Diberder, Comp. Phys. Comm. **75** (1993) 191.

[22] N. Brown and W.J. Stirling, Z. Phys. **C53** (1992) 629.

[23] CDF Collaboration, F. Abe *et al.*, Phys. Rev. Lett. **75** (1995) 4358.

[24] OPAL Collab., G. Alexander *et al.*, Phys. Lett. **B370** (1996) 185.

[25] F.A. Berends and R. Pittau, Lorentz Institut Leiden, INLO-PUB 12/91 (1991).

[26] J. Ellis, J. L. Lopez, and D. V. Nanopoulos, CERN-TH/95-314, hep-ph/9512288 (1995).